

# A Facile Route to ZnS–Polymer Nanocomposite Optical Materials with High Nanophase Content via $\gamma$ -Ray Irradiation Initiated Bulk Polymerization\*\*

By Changli Lü, Yuanrong Cheng, Yifei Liu, Feng Liu, and Bai Yang\*

Studying the fabrication and composition of semiconductor nanoparticles in polymer matrices has attracted the interest of many scientists because nanoparticle–polymer composites may find applications in high-refractive-index materials,<sup>[1]</sup> light-emitting diodes,<sup>[2]</sup> photocatalysts,<sup>[3]</sup> photovoltaic solar cells,<sup>[4]</sup> and nonlinear optical devices.<sup>[5]</sup> Control of the nanoparticle size and size distribution as well as the dispersion homogeneity in the polymer matrix are critical prerequisites for controlling the properties of the composites. However, nanoparticles are prone to aggregation in the polymer because of their high specific surface energies and inherently hydrophilic character. Therefore, it is still a technological challenge to incorporate inorganic nanoparticles into polymer matrices and thus to prepare transparent bulk nanocomposites with high nanoparticle content.<sup>[6]</sup> Far fewer studies of nanoparticle–polymer bulk materials have been reported than of nanocomposite films. Semiconductor nanoparticles (PbS, CdSe, CdTe) have been introduced into bulk polymer matrices to prepare bulk nanocomposites,<sup>[7]</sup> although the content of inorganic particles was low (<5 wt %). In these studies, two main approaches have been developed: in situ formation of nanoparticles in a presynthesized polymer and bulk polymerization of an organic monomer in the presence of premade nanoparticles. The latter provides full synthetic control over both the nanoparticles and the matrices, and is a more effective and practical route for fabricating bulk polymer nanocomposites on a large scale.

We have utilized UV radiation curing to prepare transparent ZnS–polymer nanocomposite films with high ZnS con-

tents from a solution mixture of premade ZnS particles and acrylate macromers.<sup>[8]</sup> This is an effective method for preparing nanocomposite films with nanoparticles dispersed homogeneously horizontally and vertically throughout the entire polymer matrix, but it is unsuitable for preparing thick bulk nanocomposites. In addition, the ZnS nanoparticles obtained by the usual method cannot be redispersed in monomer or solvent because of their incomplete surface modification with organic molecules. The application of  $\gamma$ -ray irradiation in the preparation of bulk polymer nanocomposites has remarkable advantages, such as processing under ambient pressure at room temperature and quick polymerization of monomers. These valuable properties can be put to use in the fabrication of nanocomposites with homogeneously dispersed inorganic nanoparticles.<sup>[9]</sup>

In this communication, we report a novel, facile route for the preparation of transparent bulk nanocomposites with high ZnS content via  $\gamma$ -ray irradiation initiated polymerization (Fig. 1). Our strategy involves the design and optimization of the nanoparticle surface and polymeric monomer as well as the selection of a suitable polymerization technology. First, we reasoned that the compatibility between nanoparticles and the polymer matrix is a prerequisite for synthesizing a bulk nanocomposite with high nanophase content. So, it is necessary to tailor the corresponding polymer matrix by the decoration of the nanoparticles with organic molecules. Furthermore, it is highly important that the monomer should act as both the ligand and solvent for the inorganic nanoparticles.<sup>[10]</sup> It has been reported that polar organic solvent molecules, such as *N,N*-dimethylformamide (DMF) and dimethyl sulfoxide (DMSO), co-ordinate to the surface of ZnS or CdS nanocrystallites and can effectively stabilize them.<sup>[11]</sup> Thus, it is expected that a monomer with a similar structure to DMF can be selected as both the solvent and ligand for the nanoparticles. Here, we have selected *N,N*-dimethylacrylamide (DMAA), which can effectively disperse and stabilize ZnS particles, as the monomer. Finally, the  $\gamma$ -ray irradiation technique is another crucial factor in the fabrication of a bulk polymer nanocomposite with high particle content. This polymerization method can induce a mild and rapid gelation process for the bulk polymeric system containing a high content of nanoparticles uniformly dispersed inside.

We present a simple approach for the large-scale production of mercaptoethanol (ME)-capped ZnS nanoparticles in DMF from Zn(OAc)<sub>2</sub> (Ac: acetate) and thiourea. The ME-

[\*] Prof. B. Yang, Dr. C. Lü, Dr. Y. Cheng, Dr. Y. Liu  
Key Lab of Supramolecular Structure & Materials  
College of Chemistry, Jilin University  
Changchun 130012 (P.R. China)  
E-mail: byangchem@jlu.edu.cn

Dr. C. Lü  
College of Chemistry, Northeast Normal University  
Changchun 130024 (P.R. China)

Dr. F. Liu  
State Key Laboratory of Polymer Chemistry and Physics  
Changchun Institute of Applied Chemistry  
Chinese Academy of Sciences  
Changchun 130022 (P.R. China)

[\*\*] This work was supported by the Program for Changjiang Scholars and Innovative Research Team in University (IRT04222) and the Science Foundation for Young Teachers of Northeast Normal University (No.111494015).

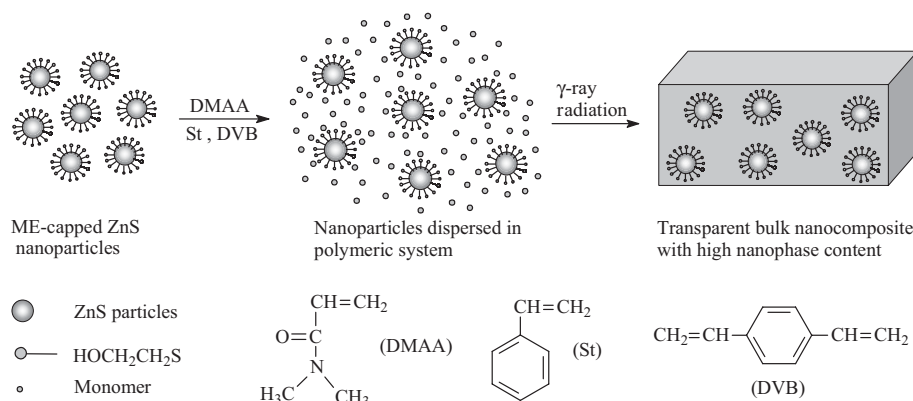


**Figure 1.** Schematic representation of the formation of transparent ZnS-polymer bulk nanocomposites with high nanophase content by  $\gamma$ -ray radiation induced polymerization of vinyl monomers. ME: mercaptoethanol; DMAA: *N,N*-dimethylacrylamide; St: styrene; DVB: divinylbenzene.

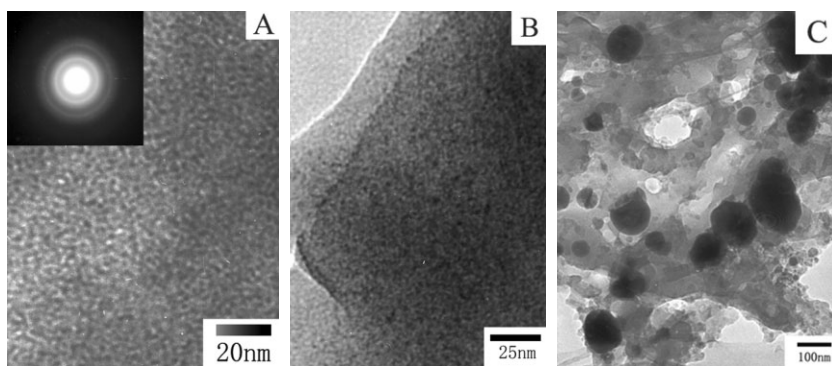
capped ZnS nanoparticles with diameters of 2–5 nm exhibit a cubic crystal structure (Fig. 2A), which is in accordance with the X-ray diffraction (XRD) results (Fig. 3, trace f). ME-capped ZnS particles can be obtained as a powder by precipitation with ethanol or acetone, and the resultant particles possess long-term stability at ambient temperature and excellent redispersibility in DMAA under ultrasonic treatment. The maximum soluble amount of ME-capped ZnS particles in DMAA can reach 80 wt %. However, poly(*N,N*-dimethylacrylamide) (PDMAA) is a water-soluble polymer.<sup>[12]</sup> For better integration of the properties of the bulk nanocomposites, styrene (St) and divinylbenzene (DVB) have been used as comonomers to obtain a crosslinked bulk nanocomposite with low humidity sensitivity. Here, the weight ratio of DMAA/St/DVB was selected as 12:5:1. When the content of capped ZnS in this polymerization system is below 60 wt %, bulk nanocomposites with good mechanical properties can be obtained after  $\gamma$ -ray irradiation.

We have successfully prepared a series of bulk nanocomposites by incorporating different amounts of ZnS nanoparticles into the mixture of monomers mentioned above, followed by  $\gamma$ -ray irradiation initiated bulk polymerization. However,

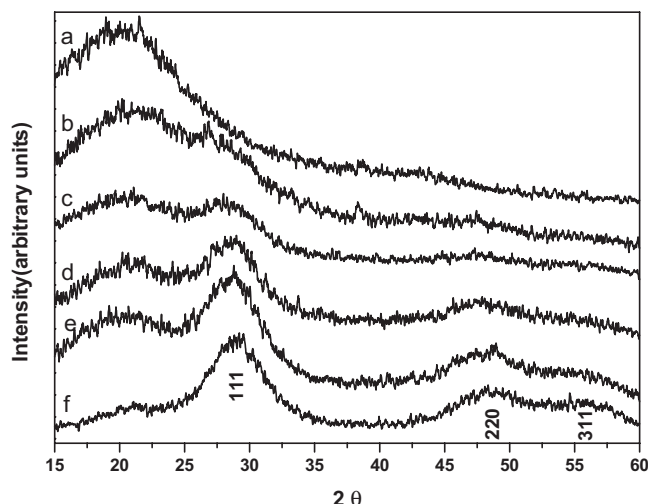
the bulk polymerization of the composite system using initiators such as 2,2'-azobisisobutyronitrile (AIBN) was unsuccessful, and especially so for polymerization systems with high contents of ZnS particles. Figure 3 presents the XRD patterns of bulk nanocomposites with different ZnS contents. The diffraction peaks corresponding to the (111), (220), and (311) planes show that the ZnS in the nanocomposite retains its zinc blende crystal structure. The intensities of these diffraction peaks gradually increase with increasing ZnS content, indicating that the ZnS particles have been successfully incorporated into the bulk polymer matrices.

Figure 4 presents the thermogravimetric analysis (TGA) results for ME-capped ZnS nanoparticles and bulk nanocomposites, as well as for the polymer matrix. The capped ZnS particles begin to decompose at about 200 °C because of the unstable ME on their surfaces, while the pristine polymer exhibits a higher initial decomposition temperature of 250 °C. As the ZnS nanoparticles are incorporated into the polymer matrix to form bulk nanocomposites under  $\gamma$ -ray radiation, the resulting nanocomposites have a similar thermal stability as the polymer matrix. However, the bulk nanocomposites show an obvious weight loss between 250 and 300 °C, which is similar to that observed in ME-capped ZnS particles. Additionally, the content of pure ZnS in the capped particles is about 66 wt %, as obtained by TGA, indicating that many capped organic molecules are present on the ZnS surface. These molecules favor the redispersion of nanoparticles in the organic monomer. The bulk-nanocomposite residue seen in the TGA curves increases with increasing ZnS content, and the amount measured is in good accordance with the calculated values of pure ZnS in the nanocomposite, based on the TGA results of capped ZnS particles.

Figure 5A shows the UV-vis transmittance spectra of the polymer matrix and the bulk nanocomposites. When the content of



**Figure 2.** Transmission electron microscopy images of A) ME-capped ZnS particles (inset: selected area electron diffraction pattern); B,C) bulk nanocomposites with 20 wt % (B) and 40 wt % (C) ME-capped ZnS particles.



**Figure 3.** XRD patterns of the polymer matrix (a); of bulk nanocomposites with 10 wt % (b), 20 wt % (c), 30 wt % (d), and 40 wt % (e) of ME-capped ZnS; ME-capped ZnS nanoparticles (f).

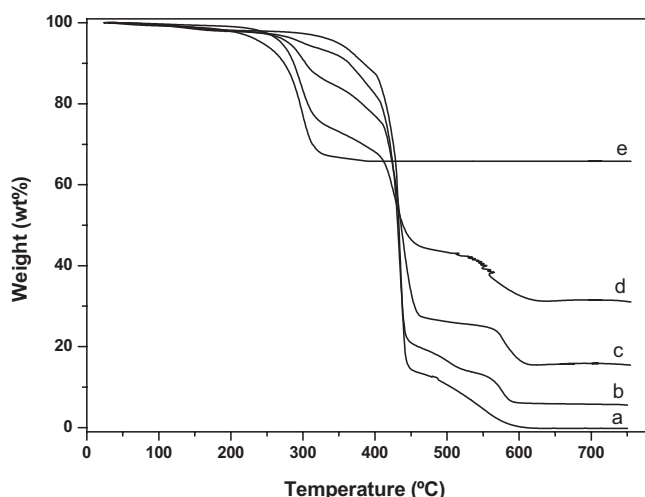
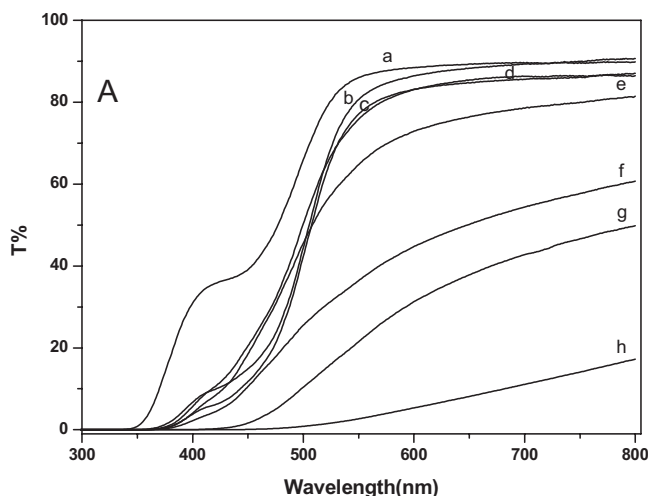


**Figure 4.** TGA curves of polymer matrix (a); of bulk nanocomposites containing 10 wt % (b), 30 wt % (c), and 50 wt % (d) capped ZnS; pure ME capped ZnS particles (e). Heating rate  $10\text{ }^{\circ}\text{C min}^{-1}$  under  $\text{N}_2$  flow.

ME-capped ZnS particles is below 30 wt %, the nanocomposites exhibit good transparency in the visible region of the electromagnetic spectrum. Figure 5B shows a photograph of the bulk nanocomposites with 20 wt % capped ZnS. The absorption between 400 and 500 nm in Figure 5A for all samples may be due to residual DVB moieties after polymerization, which are disadvantageous for the transparency of nanocomposites; however, by incorporating other monomers as crosslinker, this shortcoming could be eliminated. When the content of capped ZnS is above 30 wt %, the transparency of the bulk nanocomposites decreases with increasing particle content because of the aggregation of nanoparticles and macroscopic phase separation. For example, nanocomposite sam-



**B**



**Figure 5.** A) UV-vis transmittance ( $T$ ) spectra of polymer matrix (a), bulk nanocomposites with ME-capped ZnS contents of 5 wt % (b), 10 wt % (c), 20 wt % (d), 30 wt % (e), 40 wt % (f), 50 wt % (g), and 60 wt % (h); B) Photograph of the bulk nanocomposites containing 20 wt % ME-capped ZnS (sample thickness: 4 mm).

ples f and g are translucent to the eye. Transmission electron microscopy studies support this result (Figs. 2B and C). ZnS nanoparticles are uniformly dispersed in the bulk nanocomposite (with a ZnS content of 20 wt %) and remain at their original size of 2–5 nm without aggregation. However, in a bulk nanocomposite with 40 wt % ZnS, the particles exhibit serious aggregation. The particle aggregates reach 100 nm in size and can result in severe optical scattering and reduced transmittance of the nanocomposites.<sup>[13]</sup>

We have examined the effect of incorporating capped ZnS particles on the refractive index of bulk nanocomposites using a W2S-1 refractometer at  $20\text{ }^{\circ}\text{C}$ . Figures 6A and B shows the change in refractive index of bulk nanocomposites versus weight percentage of ME capped ZnS particles and versus volume percentage of ZnS, respectively. The volume ratios have been calculated from the weight ratios using densities of  $\rho_{\text{org}} = 1.1\text{ g cm}^{-3}$  for the organic component and  $\rho_{\text{ZnS}} = 4.1\text{ g cm}^{-3}$  for cubic ZnS crystals. Here, the densities ( $\rho_{\text{polymer}} = 1.09\text{ g cm}^{-3}$ ,  $\rho_{\text{ME}} = 1.11\text{ g cm}^{-3}$ ) and refractive indices ( $n_{\text{polymer}} = 1.54$ ,  $n_{\text{ME}} = 1.50$ ) of the polymer matrix and

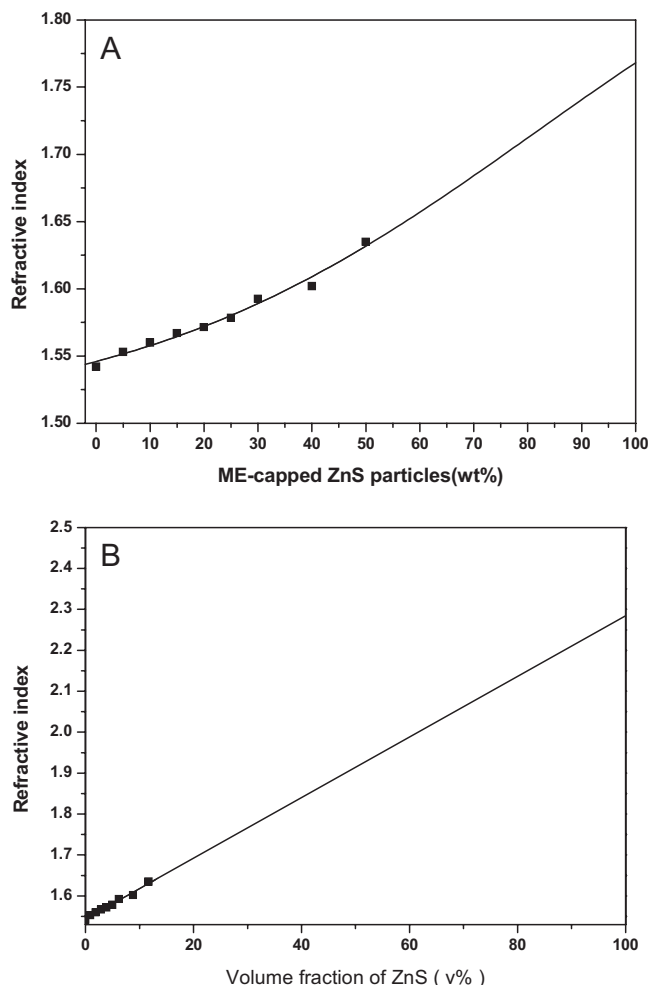


**Figure 6.** Refractive indices of ZnS-polymer bulk nanocomposites at A) different weight fractions of ME-capped ZnS particles and B) volume fractions of ZnS.

ME capping agent are considered to be in the same range. The refractive index of the bulk nanocomposites increases with increasing ZnS content. When 50 wt % capped ZnS is introduced into the polymer, the refractive index of the obtained bulk nanocomposite can reach 1.63, compared with 1.54 of the polymer matrix. This result indicates that ZnS nanoparticles contribute significantly to the increase in the refractive index of the nanocomposites.<sup>[14]</sup> The refractive index of ME-capped ZnS nanoparticles is calculated to be about 1.77 by regression analysis of the trace in Figure 6A. This refractive-index value is lower than that of bulk ZnS (2.368) because of the existence of many ME molecules on the ZnS surface, which have a low refractive index. Figure 6B illustrates the linear relationship between the refractive index of nanocomposites and the volume fraction of ZnS (within experimental error). A linear dependence of the refractive index on the volume fraction of the incorporated particles has also been found in other systems.<sup>[1b,15]</sup> The refractive index of pure ZnS has been calculated to be 2.283 from Figure 6B by regres-

sion analysis for an extrapolation to 100 vol % ZnS. It can be seen that the refractive index of ZnS obtained from the nanocomposites is smaller but close to the value of bulk ZnS, within experimental error. Suter and coworkers have found that the refractive index of small-sized PbS particles was significantly lower than that of the bulk material because of the size-quantization effect.<sup>[16]</sup> However, ZnS is a wide-bandgap semiconductor, and its Bohr diameter is about 5.5 nm.<sup>[17]</sup> For our systems, the size of ZnS particles (2–5 nm) is close to their Bohr diameter. So, it is possible that in the refractive index of ZnS, quantum-size effects are not evident, unlike in PbS nanoparticles.<sup>[16]</sup>

In summary, we have provided a simple and effective method for the preparation of transparent bulk nanocomposites with high nanophase content through the appropriate design and tailoring of nanoparticles and monomer. This novel strategy can be applied not only to the preparation of bulk nanocomposites containing ZnS particles but also to other composite systems containing, for example, CdS or core/shell particles. In addition, the surface of the highly dispersed nanoparticles can be grafted with double bonds or capped with mixed ligands to obtain covalently linked bulk nanocomposites. Such bulk nanocomposites can be potentially used to fabricate multifunctional devices or optical materials with tunable refractive indices.

## Experimental

The ME-capped ZnS nanoparticles were synthesized in DMF according to a modified literature procedure [17]. Zinc acetate (0.1 mol), thiourea (0.118 mol), and ME (0.148 mol) were dissolved in 100 mL DMF. The solution was refluxed at 160 °C for 10 h under nitrogen. 300 mL of acetone or ethanol was then added, and a flocculent precipitate formed that was separated by centrifugation. The white powder was thoroughly washed several times with methanol and then vacuum-dried ( $5 \times 10^{-2}$  Pa). The ME-capped ZnS powder was found to dissolve readily in DMF and DMAA.

The desired amount (in wt %) of ME-capped ZnS powder was dispersed in the monomer mixture of DMAA, St, and DVB under sonication. The weight ratio of DMAA/St/DVB was selected to be 12:5:1. After degassing, the transparent composite systems were poured into glass-plate molds (10 cm  $\times$  6 cm  $\times$  4 mm). The filled glass molds were sealed in a plastic bag under vacuum and then subjected to  $\gamma$ -ray irradiation. Irradiation was performed with a  $^{60}\text{Co}$  source ( $7 \times 10^4$  Ci,  $1 \text{ Ci} = 3.7 \times 10^{10} \text{ Bq}$ ) with a dose rate of  $8.31 \text{ kGy h}^{-1}$ . The irradiation temperature was in the range of 25–30 °C. Thereafter, the samples were postcured at 150 °C for 2 h.

Received: November 10, 2005

Final version: January 6, 2006

- a) F. Papadimitrakopoulos, P. Wisniecki, D. E. Bhagwagar, *Chem. Mater.* **1997**, 9, 2928. b) L. Zimmermann, M. Weibel, W. Caseri, U. W. Suter, *J. Mater. Res.* **1993**, 8, 1742. c) C. Lü, C. Guan, Y. Liu, Y. Cheng, B. Yang, *Chem. Mater.* **2005**, 17, 2448.
- a) V. L. Colvin, M. C. Schlamp, A. P. Alivisatos, *Nature* **1994**, 370, 354. b) A. A. Mamedov, A. Belov, M. Giersig, N. N. Mamedov, N. A. Kotov, *J. Am. Chem. Soc.* **2001**, 123, 7738.
- a) S. Shiojiri, T. Hirai, I. Komasaawa, *Chem. Commun.* **1998**, 1439. b) T. Hirai, T. Watanabe, I. Komasaawa, *J. Phys. Chem. B* **2000**, 104, 8962.

- [4] a) T. Hasobe, H. Imahori, P. V. Kamat, T. K. Ahn, S. K. Kim, D. Kim, A. Fujimoto, T. Hirakawa, S. Fukuzumi, *J. Am. Chem. Soc.* **2005**, *127*, 1216. b) R. A. J. Janssen, M. M. Wienk, *Adv. Mater.* **2004**, *16*, 1009.
- [5] V. I. Klimov, S. Mikhailovsky, S. Xu, A. Malko, J. A. Hollingsworth, C. A. Leatherdale, H. Eisler, M. G. Bawendi, *Science* **2000**, *290*, 314.
- [6] a) F. M. Pavel, R. A. Mackay, *Langmuir* **2000**, *16*, 8568. b) C. H. Hung, W. T. Whang, *J. Mater. Chem.* **2005**, *15*, 267. c) W. Caseri, *Macromol. Rapid Commun.* **2000**, *21*, 705.
- [7] a) M. Gao, Y. Yang, B. Yang, F. Bian, J. Sheng, *Chem. Commun.* **1994**, 2779. b) J. Lee, V. C. Sundar, J. R. Heine, M. G. Bawendi, K. F. Jensen, *Adv. Mater.* **2000**, *12*, 1102. c) L. Erskine, T. Emrick, A. P. Alivisatos, J. M. Fréchet, *Polym. Prepr.* **2000**, *41*, 593. d) H. Zhang, Z. Cui, Y. Wang, K. Zhang, X. Ji, C. Lü, B. Yang, M. Gao, *Adv. Mater.* **2003**, *15*, 777.
- [8] C. Lü, Z. Cui, Y. Wang, Z. Li, C. Guan, B. Yang, J. Sheng, *J. Mater. Chem.* **2003**, *13*, 2189.
- [9] a) Y. Zhu, Y. Qian, X. Li, M. Zhang, *Chem. Commun.* **1997**, 1081. b) Y. Xie, Z. Qiao, M. Chen, X. Liu, Y. Qian, *Adv. Mater.* **1999**, *11*, 1512. c) X. Jiang, Y. Xie, J. Lu, L. Zhu, W. He, Y. Qian, *Chem. Mater.* **2001**, *13*, 1213.
- [10] J. H. Golden, H. B. Deng, F. J. DiSalvo, J. M. J. Fréchet, P. M. Thompson, *Science* **1995**, *268*, 1463.
- [11] a) H. Hosokawa, K. Murakoshi, Y. Wada, S. Yanagida, M. Satoh, *Langmuir* **1996**, *12*, 3598. b) H. Hosokawa, H. Fujiwara, K. Murakoshi, Y. Wada, S. Yanagida, M. Satoh, *J. Phys. Chem.* **1996**, *100*, 6649. c) S. K. Haram, M. E. Wankhede, *Chem. Mater.* **2003**, *15*, 1296.
- [12] a) K. Haraguchi, R. Farnworth, A. Ohbayashi, T. Takehisa, *Macromolecules* **2003**, *36*, 5732. b) V. Bekiari, K. Pagonis, G. Bokias, P. Lianos, *Langmuir* **2005**, *20*, 7972.
- [13] L. L. Beecroft, C. K. Ober, *Chem. Mater.* **1997**, *9*, 1302.
- [14] C. Lü, Z. Cui, Z. Li, B. Yang, J. Sheng, *J. Mater. Chem.* **2003**, *13*, 526.
- [15] a) L. Zimmermann, M. Weibel, W. Caseri, U. W. Suter, P. Walther, *Polym. Adv. Technol.* **1993**, *4*, 1. b) R. J. Nussbaumer, W. R. Caseri, P. Smith, T. Tervoort, *Macromol. Mater. Eng.* **2003**, *288*, 44. c) C. Lü, Z. Cui, C. Guan, J. Guan, B. Yang, J. Shen, *Macromol. Mater. Eng.* **2003**, *288*, 717. d) E. J. A. Pore, M. Asami, J. D. Mackenzie, *J. Mater. Res.* **1989**, *4*, 1016.
- [16] T. Kyprianidou-Leodidou, W. Caseri, U. W. Suter, *J. Phys. Chem.* **1994**, *98*, 8992.
- [17] J. Nanda, S. Sapra, D. D. Sarma, *Chem. Mater.* **2000**, *12*, 1018.